Applications of magnetic circular dichroism spectroscopy to porphyrins and phthalocyanines

Nagao Kobayashi* and Katsunori Nakai

Received (in Cambridge, UK) 2nd April 2007, Accepted 11th May 2007
First published as an Advance Article on the web 13th June 2007
DOI: 10.1039/b704991a

Magnetic circular dichroism (MCD) spectroscopy has widely been applied to porphyrins and phthalocyanines since around 1970, in order to elucidate their electronic structures. In this mini-review, some representative MCD results from the author's laboratory over the past 30 years are introduced, together with recent results from other laboratories. MCD studies on the following monomeric species are included: D_{4h} type, adjacent *vs.* opposite type diaromatic ring-fused, non-planar, and reduced and oxidized species, as well as species showing temperature-dependent MCD signals. In addition, one example illustrates the use of MCD as a probe for the distal histidine residue in myoglobin. Recent results on dimers and oligomers are also reported. In particular, it is confirmed that the spectra of cofacial eclipsed dimers do not reflect the molecular symmetry of the constituent monomers. The spectra of rare-earth sandwich dimers and trimers are definitively assigned. Using spectra of planar oligomers of porphyrins, it is reiterated that it is often dangerous to assign the absorption bands of chromophores based only on the results of molecular orbital calculations. Some examples show that MCD can give information on the relative size of the ΔHOMO (energy difference between the HOMO and HOMO−1) and ΔLUMO (energy difference between the LUMO and LUMO+1); for example, if ΔHOMO > ΔLUMO, the MCD signal changes from minus to plus in ascending energy.

Introduction

Magnetic circular dichroism (MCD) spectroscopy was first applied to porphyrin compounds from approximately 1970,[1] together with the development of CD instrumentation. Although this spectroscopy was also widely used in the analysis of electronic states of metallocomplexes[2] and some

Department of Chemistry, Graduate School of Science, Tohoku University, Sendai 980-8578, Japan.
E-mail: nagaok@mail.tains.tohoku.ac.jp

Nagao Kobayashi

Professor Nagao Kobayashi was born in Nagano, Japan, where the Winter Olympic Games were held in 1998, on January 21, 1950. He received his DSc in 1978 on the magnetic circular dichroism (MCD) of catalase and peroxidase and Doctor of Pharmacy in 1986 on the electrocatalytic reduction of oxygen using water-soluble porphyrins and phthalocyanines, both from Tohoku University. He was appointed as a research associate of the Chemical Research Institute of Non-Aqueous Solutions and subsequently of Pharmaceutical Institute of Tohoku University in 1983 and 1985, respectively. After spending one month as an associate professor of the above Pharmaceutical Institute, he has been a full professor of the Department of Chemistry, Graduate School of Science, Tohoku University since April of 1995. He spent time as a visiting professor in the laboratories of Professors A. B. P. Lever in Toronto, Canada, and J. Simon in ESPCI, Paris, where Pierre and Marie Curie discovered radium in 1898. He has been acting as the Secretary of the Society of Porphyrins and Phthalocyanines since 2000, and received the Chemical Society of Japan Award for Creative Work. His research interest is the chemistry of giant aromatic molecules which show interesting spectroscopic (particularly absorption, MCD and CD) properties.

Katsunori Nakai

Katsunori Nakai was born in Gunma, Japan in 1977. He received his BS degree from Tohoku University in 2000. In 2005, he received his PhD degree from the same university under the supervision of Profs. Hirohiko Kono and Yuichi Fujimura. Since August of 2006, he has been a COE fellow of Tohoku University working with Prof. Nagao Kobayashi. His current research fields are theoretical studies of the electronic structure of nano-sized compounds and of the dynamics of molecules in laser fields.

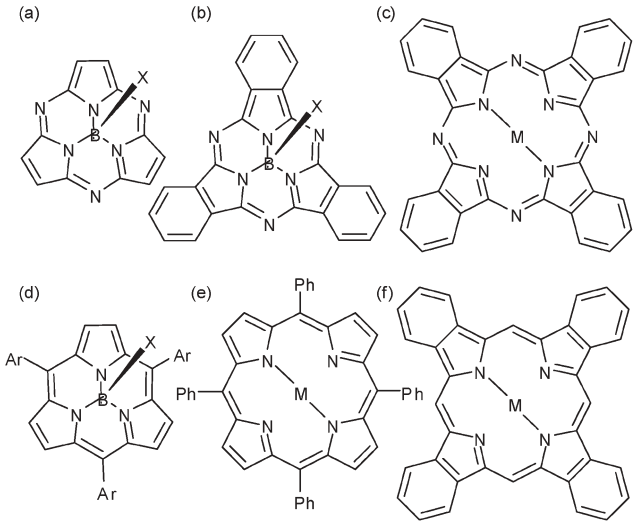

Fig. 1 Structures of some representative porphyrins in this review: (a) subtriazaporphyrin, (b) subphthalocyanine, (c) phthalocyanine, (d) *meso*-triarylsubporphyrin, (e) *meso*-tetraphenylporphyrin, (f) tetrabenzoporphyrin.

smaller aromatic compounds,[3] its coming of age occurred through the study of porphyrins, which may be related to the diversity of functions of natural porphyrins. In addition, the shape and extent of deformation of synthetic porphyrins can be modified by introducing substituent groups or by changing the shape of their π systems.[4] This kind of structural and functional diversity of porphyrins may be the reason why MCD spectroscopy has been intensively used by porphyrin researchers. In this review, we describe how MCD is effective in analyzing the electronic states of porphyrins and phthalocyanines, showing some recent typical examples. Fig. 1 shows the basic structures of the porphyrinic compounds referred to in this study.

Qualitative information obtained from MCD spectroscopy

MCD spectra are obtained for almost all aromatic molecules by setting a magnet in a circular dichroism (CD) spectrodichrometer. However, in contrast to CD spectroscopy, the compounds need not be optically active, and the analysis of MCD spectra gives information on electronic states, in particular, excited states. The MCD signal arises from the same transitions as those seen in the UV-visible absorption spectrum, but the selection rules are different, since the intensity mechanism depends on the magnetic dipole moment in addition to the dipole moment which normally determines the UV-visible absorption intensity. MCD spectroscopy is, therefore, complementary to UV-visible absorption spectroscopy, as it can provide ground and excited state degeneracy information essential in understanding the electronic structure of molecules of high symmetry. The specificity of the MCD technique arises from three highly characteristic spectral features. Fig. 2 shows how each of the three spectral features that characterize the MCD spectrum, *i.e.* the Faraday *A*, *B* and *C* terms arise.[5] A derivative-shaped band, the so-called

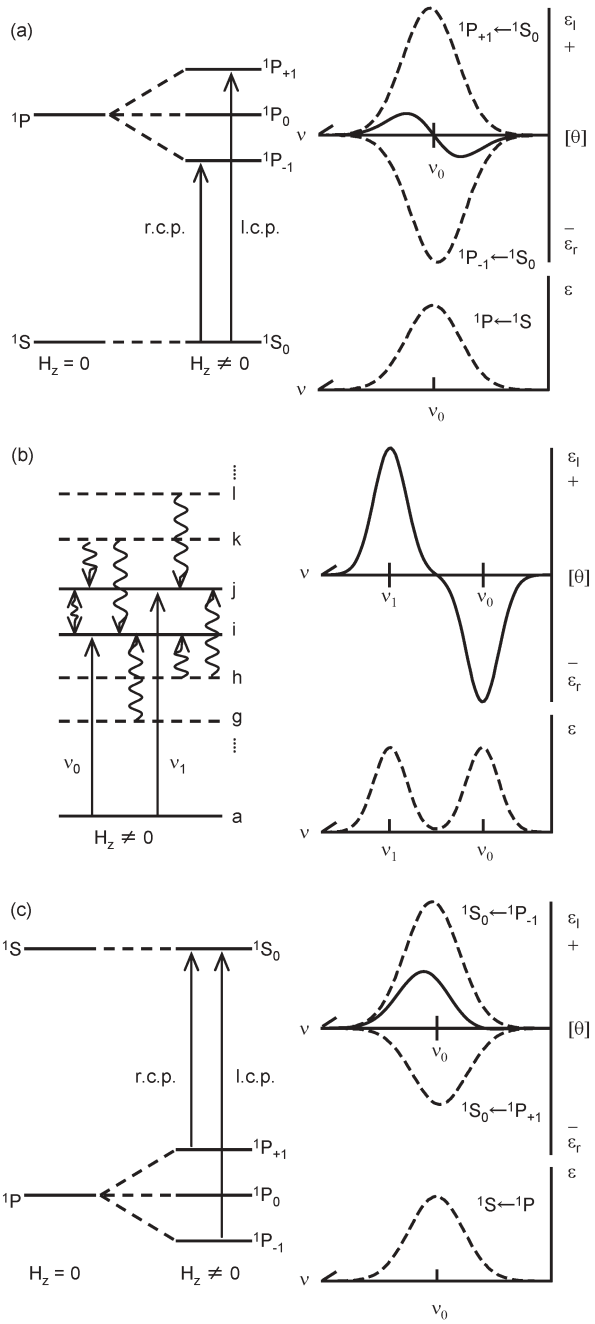

Fig. 2 Effect of magnetic field on atomic ^1S and ^1P states and selection rules for circularly polarized light for (a) $^1P \leftarrow {}^1S$ and (c) $^1S \leftarrow {}^1P$ transitions, producing Faraday *A* and *C* terms, respectively. The *A* term arises from the Zeeman splitting of an orbitally degenerate excited state, while the *C* term arises from the Boltzmann population distribution across the degenerate ground state. (b) Faraday *B* terms arise from second order effects based on field-induced mixing of the zero-field states *via* magnetic dipole transition moments.

Faraday *A* term of either positive sign (positive lobe to higher energy of the crossover point) or negative sign (positive lobe to lower energy of the crossover point) appears when the excited states are orbitally degenerate, associated with absorption peaks. Thus, Faraday *A* terms are generally predicted only when the molecule possesses at least a three-fold axis of symmetry. Faraday *B* terms, *i.e.* Gaussian-shaped bands of

either positive or negative sign, are observed when an excited state is mixed with nearby transitions by the magnetic field, and have integral-type envelopes near the relevant absorption peaks. Interacting *B* terms give spectral envelopes of opposite sign. Therefore, in the case of D_{2h} or metal-free porphyrinoids, the two *B* terms lying under the two absorption components indicate that these are the symmetry-split *x* and *y* polarized transitions. When the energy splitting of the *x* and *y* polarized transitions is small, the observed MCD curve appears like a Faraday *A* term (this is called a pseudo-*A* term). However, the difference from the *A* term is that the negative and positive envelope positions are close to the two absorption peaks. Faraday *C* terms appear when the ground state is orbitally degenerate. Its shape is close to that of the Faraday *B* term, but its intensity is inversely proportional to the absolute temperature. Thus *C* terms have often been observed in organic radicals and metal complexes. Temperature dependence of the spectral intensities arises from the change in Boltzmann distribution across the split orbital components of the degenerate ground state. The shape of the *C* term is the same as a *B* term, that is a Gaussian-shaped positive or negative envelope is observed near the absorption maxima. Faraday parameters can occur with either sign, unlike absorption coefficients. Normal porphyrins consisting of four pyrrole rings can be approximated as molecules having D_{2h} (metal-free species) and D_{4h} or D_{4d} (metallated species) symmetry, so that normal metalloporphyrins generally show dispersion type MCD curves corresponding to the Q and Soret (or B) absorption peaks. In addition, MCD gives information with respect to the relative size of ΔHOMO (energy difference between the HOMO and HOMO−1) and ΔLUMO (energy difference between the LUMO and LUMO+1). If ΔHOMO > ΔLUMO, the sign of the spectrum changes from minus to plus in ascending energy. Since, in normal metalloporphyrins, the LUMO is doubly degenerate, the sign changes from minus to plus in ascending energy.

1 Monomeric species

(A) D_{4h} type species. In order to show the validity of MCD spectroscopy, Fig. 3 shows absorption and MCD spectra of magnesium octaphenyltetraazaporphyrin in pyridine.[6] In both the Q and Soret band regions, positive Faraday *A* MCD terms are observed, in accordance with double degeneracy in the excited states. Noteworthy is the appearance of a dispersion type *A* term lying at the longer wavelength tail of the Soret band at around 460 nm. A similar, but much weaker Faraday *A* term was detected as early as 1987 for ZnPc coordinated by imidazole, at the longer wavelength side of the normally accepted Soret band by the MCD technique.[7] These bands were detected for the first time by MCD, and assigned to a π–π* transition to degenerate excited states. Even if the absorption is very weak and its position is not clear, the energy of these transitions can be determined easily, since *A* terms are derivative-shaped, as seen in Fig. 2.

(B) *Adjacent vs. opposite* type diaromatic ring-fused azaporphyrin derivatives. We can fuse two aromatic rings at the adjacent or opposite two pyrrole rings, to yield compounds of

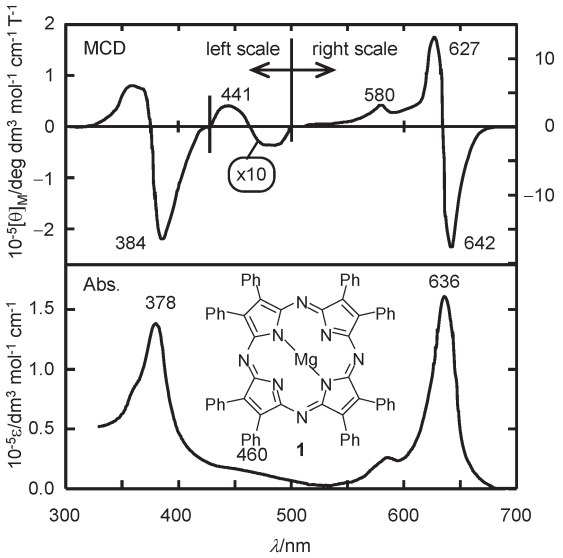

Fig. 3 Absorption and MCD spectra of **1** in pyridine (redrawn from ref. 6).

approximately C_{2v} and D_{2h} symmetry, respectively.[8] In the case of adjacently-disubstituted C_{2v} symmetry compounds, the Q band does not split, or the splitting is very small, if at all, because of the pseudo-degeneracy.[9,10] This feature is well recognized by comparing the absorption and MCD of a series of compounds in Fig. 4. In C_{2v} type compounds, the Q absorption bands do not split and derivative-shaped MCD curves were observed, corresponding to the Q peaks. In D_{2h} type compounds, however, the Q band splits and the extent of splitting increases with increasing ratio of the long and short axis (although the Q band of oppositely-dibenzo-substituted compounds in this figure appears not to split, this is due to the effect of substituents introduced into the periphery in order to increase solubility). When the splitting is small, a Faraday *A* term type curve is seen in the Q band region. However, this is a pseudo-Faraday *A* term resulting from a small splitting of the Q band. As mentioned above, in this case, the positions of the Q MCD trough and peak correspond approximately to the split absorption peak. In the two naphthalene-fused compounds, four Q peaks are seen in the absorption spectra. From the absorption spectra alone, we cannot determine which of the peaks at 705 and 688 nm corresponds to the split component. For this question, MCD spectra gives the answer that it is possibly the 705 nm peak, since a negative envelope (*B* term) is seen associated with the absorption band at 763 nm (note that interacting *B* terms give opposite signs). In anthracene-fused compounds, the splitting becomes larger. Thus, we can use MCD characteristics in determining the molecular symmetry of a compound. For example, a zinc tetraazaporphyrin (TAP)[11] fused with two naphthalene units was synthesized,[8a] which was a structural isomer of phthalocynine (Pc)[11] with respect to the π system. This exhibited split Q absorption peaks at 806, 726 and 647 nm, and in MCD spectra, negative, negative and positive envelopes (*B* terms) were detected in the above order of peaks (Fig. 5). Although X-ray analysis was not provided, we can confirm that it is a oppositely-disubstituted compound from the two findings that

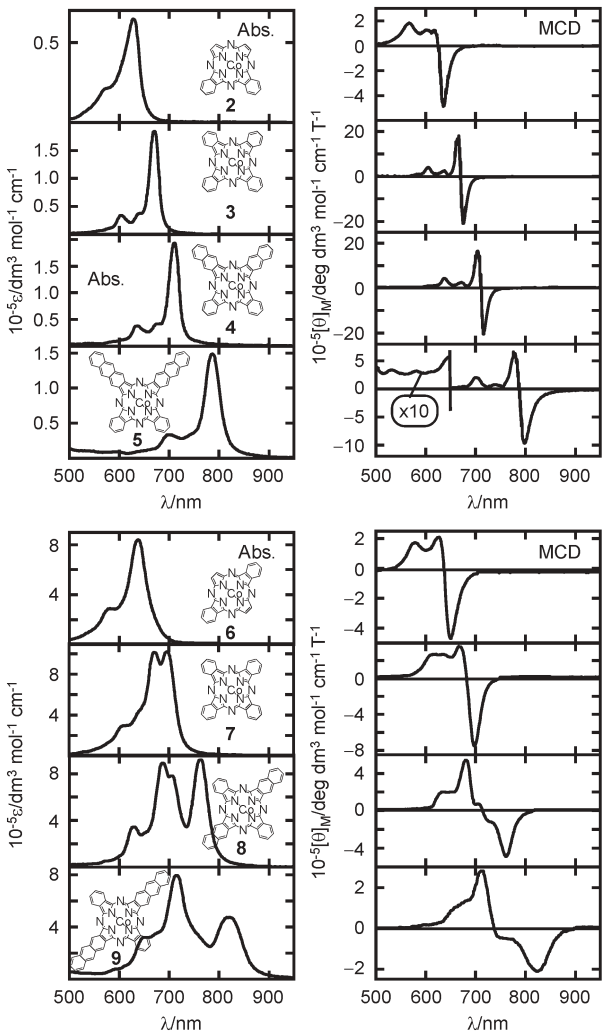

Fig. 4 Absorption (left) and MCD (right) spectra of adjacently diaromatic ring-fused **2–5** and oppositely diaromatic ring-fused **6–9** in toluene (redrawn from ref. 8*d*). In the absorption spectra of **6** and **7**, the Q band is either not split (the former) or split (the latter). These are due to substituent effects on the periphery (not drawn).

(i) a large degree of splitting was observed and (ii) *B*-terms of opposite signs appeared.

Very extreme cases of adjacent and opposite compounds were reported for reduced TAPs (Fig. 6).[12] In these compounds, two pyrrole rings of the TAPs are reduced, and adjacent and opposite type compounds are, respectively, called tetraazaisobachteriochlorin and tetraazabachteriochlorin. In the former case, the splitting of the Q band is so small that simultaneous band-deconvolution of both the absorption and MCD spectra was required to determine the position of the split component. In the latter case, the splitting is very large, but we can easily understand that the 513 nm band is the split component, since the sign of MCD envelope is opposite to that at the band at *ca.* 880 nm. The MCD intensity of the 880 nm band is weak, since it is far from the interacting band (*i.e.* the band at 513 nm). Although the MCD intensity of the 513 nm band is strong, this is due to intensity borrowing from the nearby Soret band.

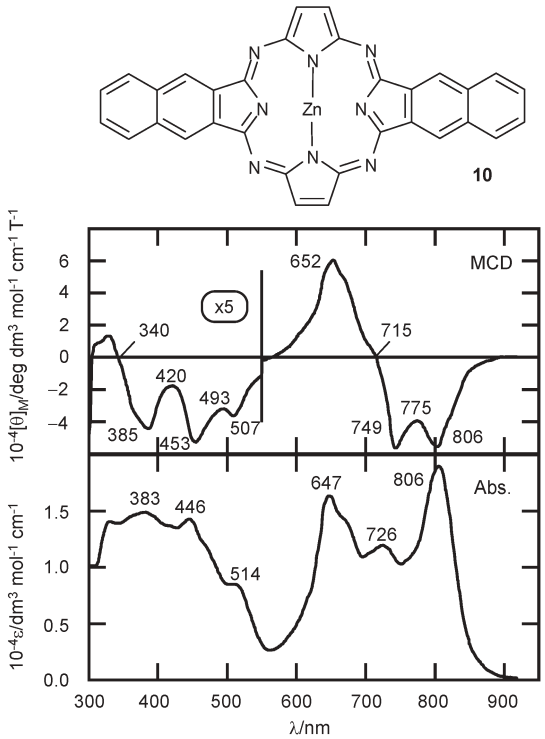

Fig. 5 Absorption and MCD spectra of **10** which is a structural isomer of phthalocyanine (redrawn from ref. 8*a*).

(C) Non-planar species. Band envelope analyses of absorption spectra may be possible. However, while estimation of the energy of the band center directly from the spectrum is useful, there is no certainty that the transitions responsible for all of the intensity actually have energies represented by the various maxima measured directly from the electronic absorption spectra. In addition, the total number of transitions often cannot be estimated with any degree of accuracy. The assignment of the absorption bands of porphyrins and Pcs of the group 6–9 elements is not easy, and MCD is virtually the only supplementary method. For example, many CT and π–π* bands of Fe(II and III)Pcs have been assigned by the simultaneous band deconvolution of absorption and MCD spectra, where bands of a fixed shape are fitted to the experimental data.[13] In this case, the energy, bandwidth, and number of the components introduced are identical or similar in the two spectra, and the number of components is reduced until the error becomes abruptly large by removing the last component. For almost-flat Fe(II) low-spin Pcs,[13*a*] the position of two MLCTs, and the Q_{00}, Q_{01}, B1 and B2 (both are the Soret bands), N and L transitions are correctly determined by this technique. Although there are no bands beyond the Q band for flat D_{4h} Fe(II) low-spin Pc, two new peaks appear beyond the Q band when the Pc plane is deformed to D_{2d} type by introducing sterically bulky substituent groups (the oxidation and spin states are the same).[14] Since the Q band is the lowest energy π–π* transition, the origin of these two bands is considered to be CT bands. Seemingly and also by band deconvolution, the presence of two transitions are postulated (Fig. 7). One at the lowest energy (930 nm) is a transition to a non-degenerate state, since a negative envelope of *B* term was

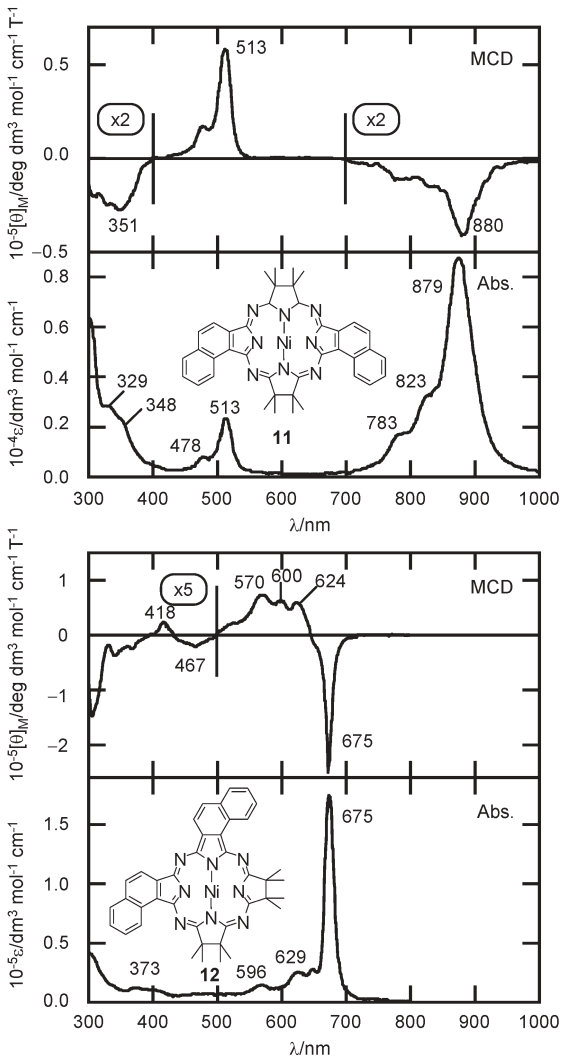

Fig. 6 Absorption and MCD spectra of opposite type **11** (top) and adjacent type **12** (bottom) (redrawn from ref. 12*c*).

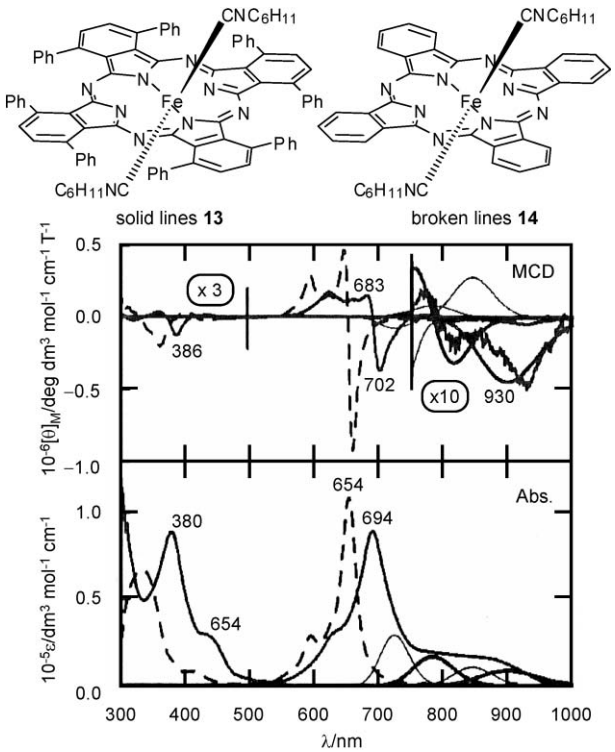

Fig. 7 Absorption and MCD spectra of **13** with D_{2d} symmetry (solid lines) and **14** with D_{4h} symmetry (broken lines) (redrawn from ref. 14). The near-IR region is band-deconvoluted.

observed corresponding to the absorption peak, while another one at higher energy (794 nm) was considered to be a transition to a degenerate excited state from the Faraday *A* term MCD curve. Next, we considered the correlation between D_{4h} and D_{2d} point groups (Scheme 1). In D_{4h} symmetry, four CT transitions are allowed, while in D_{2d} symmetry two more CT transitions ($e \rightarrow e(\pi)$ and $b_2(b_1) \rightarrow e(\pi)$) become allowed transitions in addition to the four CT transitions, and Faraday

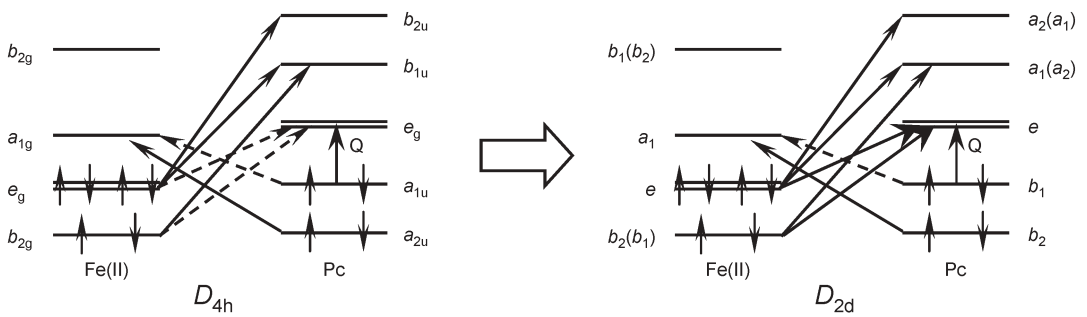

transition	CT	polarization	MCD
$a_{2u} \rightarrow a_{1g}$	L→M	Z	B
$a_{1u} \rightarrow a_{1g}$	L→M	forbidden	
$b_{2g} \rightarrow b_{1u}$	M→L	Z	B
$e_g \rightarrow b_{1u}, b_{1g}$	M→L	XY	B
$e_g \rightarrow e_g$	M→L	forbidden	
$b_{2g} \rightarrow e_g$	M→L	forbidden	

transition	CT	polarization	MCD
$b_2 \rightarrow a_1$	L→M	Z	B
$b_1 \rightarrow a_1$	L→M	forbidden	
$b_2(b_1) \rightarrow a_1(a_2)$	M→L	Z	B
$e \rightarrow a_1(a_2), a_2(a_1)$	M→L	XY	A
$e \rightarrow e$	M→L	Z	B
$b_2(b_1) \rightarrow e$	M→L	XY	A

Scheme 1 Possible transitions for iron(II) low-spin porphyrinoids in D_{4h} and D_{2d} symmetry. Solid lines and broken lines indicate allowed and forbidden transitions, respectively.

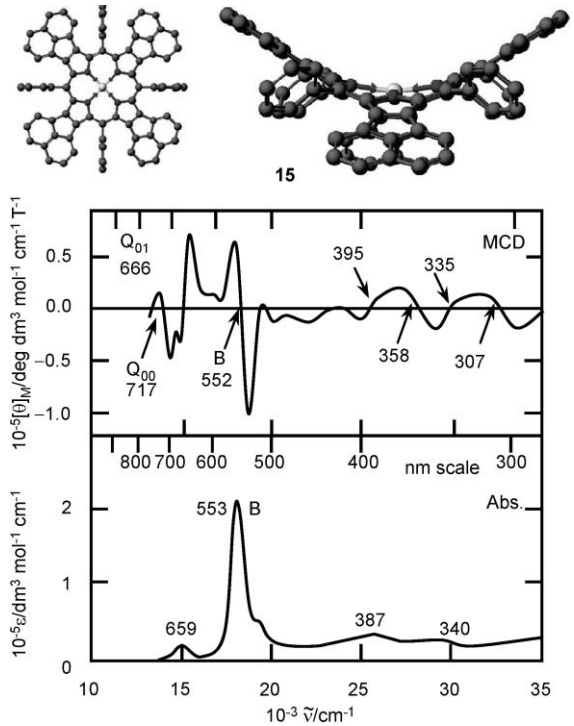

Fig. 8 Absorption and MCD spectra of **15** with D_{2d} symmetry (redrawn from ref. 15).

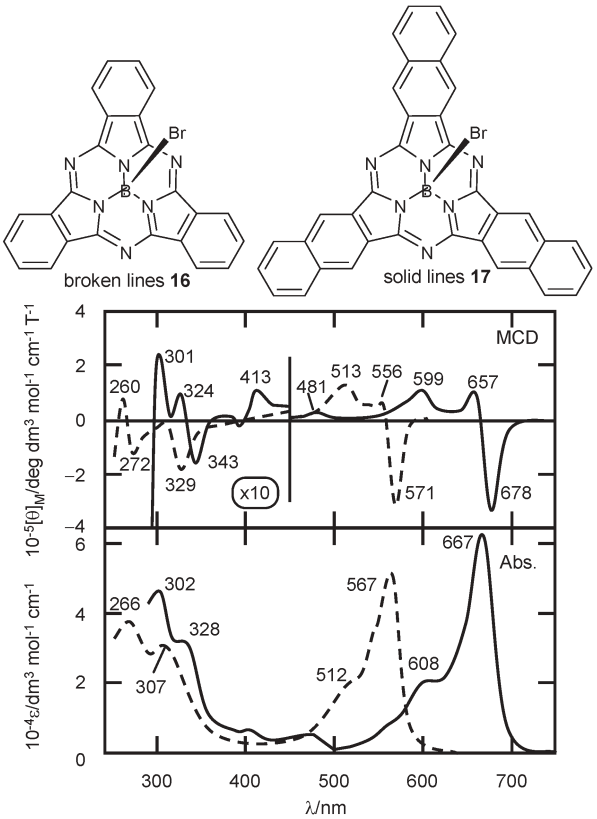

Fig. 9 Absorption and MCD spectra of **16** (broken lines) and **17** (solid lines) with C_{3v} symmetry (redrawn from ref. 16*b*).

B- and *A*-terms, respectively, are expected in the MCD spectrum. The bands deconvoluted at 784 and 930 nm are, therefore, assigned to be the *XY*-polarized $b_2(b_1) \rightarrow e(\pi)$ (Faraday *A* term) and *Z*-polarized $e \rightarrow e(\pi)$ (*B* term) MLCT transitions, respectively. In this way, we can assign absorption bands only if we have a primitive knowledge of MCD spectroscopy.

In the case of metal porphyrinoids with symmetric perimeters, negative *A* terms have rarely been observed. Recently, negative *A* terms were seen, corresponding to the Q_{00} and Soret (B) bands of zinc tetraphenyltetraacenaphthoporphyrin (Fig. 8), suggesting that $\Delta LUMO \cong \Delta HOMO \approx 0$.[15] Furthermore, careful inspection of these two negative *A* terms suggested that they result from a structural perturbation which is symmetric with respect to the 4-fold axis of symmetry of the $C_{16}H_{16}^{2-}$ parent cyclic perimeter (*i.e.* folding of the ligand) and which disrupts the orbital angular momentum properties of the LUMO to a greater extent than those of the HOMO. This conclusion could not be obtained from either ^{1}H NMR or UV-visible absorption spectroscopy.

Ring-contracted azaporphyrinoids consisting of three pyrrole derivatives called subazaporphyrins (subAP), subphthalocyanines (subPcs), and subnaphthalocyanines (subNcs), all show peculiar Q MCD curves (Fig. 9).[16] That is, although Faraday *A* terms are observed consistent with the presence of a C_3 rotation axis, the positive lobe at higher energy always appears smaller than the negative lobe at lower energy, which may be due to a superimposition of −ve/+ve vibrational MCD at higher energy. In addition, a positive broad MCD peak (*B*-term) is always observed at higher energy (513 and 599 nm MCD peaks). Although the reason for this positive *B* term was not pointed out when the papers on these compounds were published, recent TD-DFT calculations clearly suggest that this *B* term may arise from a *z*-polarized transition due to a cone-shaped structure.[17] Without MCD spectroscopy, this *z*-polarized transition may not have been found, since the absorption spectrum corresponding to this region looks like vibrational bands of the Q_{00} band.

Subporphyrins (subPs) are cyclic trimers of pyrrole connected by three methine carbon atoms. They also have domed structures similar to subAP, subPc and subNc, but their absorption spectra are closer to those of porphyrins, since carbon atoms occupy the *meso* positions. They have weak Q and intense Soret (B) bands as with normal porphyrins. The Soret MCD behavior of triarylsubPs is very unusual in that the sign of the Faraday *A* term changes depending on the electron-donating or -withdrawing property of *meso*-aryl substituents.[18] When electron-donating aryl groups are used, the MCD signal is a normal *A* term which changes −ve/+ve in ascending energy, while in contrast, it is a negative *A* term (+ve/−ve) when an electron-withdrawing group is introduced (Fig. 10). The reason for this abnormal behavior has not been elucidated, although the interaction between the *meso*-aryl group and the subP core is conjectured to be larger than that between the *meso*-aryl groups and the TPP core.

(D) Reduced and oxidized species. It is difficult to obtain stable reduced species of porphyrins, since the methine carbon bridges linking the pyrrole rings are readily reduced through protonation to form phlorin complexes, although chemical

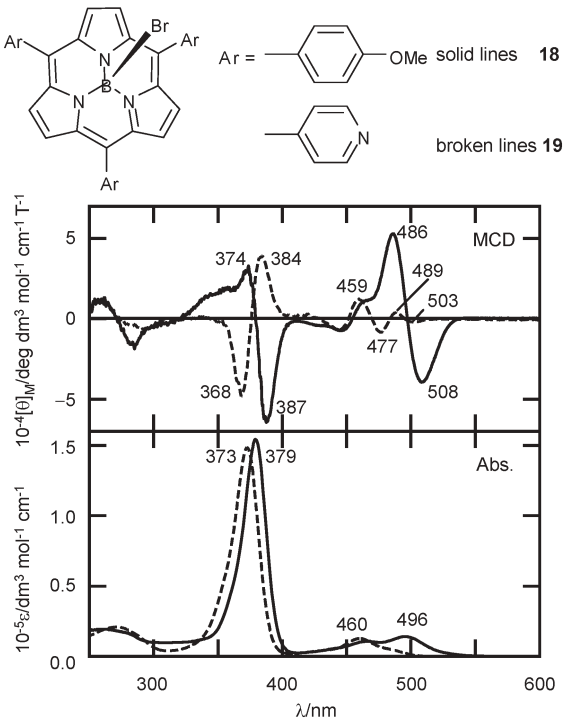

Fig. 10 Absorption and MCD spectra of **18** (solid lines) and **19** (broken lines) with approximate C_{3d} symmetry (our unpublished data and redrawn from ref. 18).

reduction using sodium benzophenone ketyl in THF[19] and hydrazine reduction in DMF,[20] and electrochemical reduction[21] have been reported. Mack and Stillman succeeded in reducing ZnPc instead of Zn porphyrin by hydrazine hydrate, and recorded its monoanionic spectra (Fig. 11).[22] This was the first complete assignment of the optical spectra of any porphyrin or Pc anion radical. From the observed plurality of MCD *B* terms, it was proposed that the combined effects of the loss of aromaticity with the addition of the 19th π-electron, Jahn–Teller distortion, and non-symmetric solvation of the ring lead to a change in molecular geometry from the D_{4h} of neutral ZnPc to C_{2v} for the ZnPc anion radical. Unlike the spectrum of diamagnetic ZnPc, the spectrum of the anion radical extended from 250 to 1000 nm (9500 to 35000 cm^{-1}) with three prominent clusters of bands, centered on *ca*. 960, 600 and 400 nm (10420, 16670 and 25000 cm^{-1}, respectively). The MCD spectrum showed recurring coupled pairs of bands in each of these regions, with no significant temperature dependence (*B* terms). Extensive band-deconvolution analysis was performed, and by comparing the results with those of molecular orbital calculations, the bands at around 960, 600 and 400 nm were assigned, respectively, as the Q, π*–π* and Soret (B1/B2) bands.

The absorption and MCD spectra of dianionic ZnPc were also analysed. However, the assignment of the bands remains problematic.[23]

Characterization of the spectra of the π-cation radical species of metalloPcs and -porphyrins is also difficult, partly because so few spectra have been reported for samples in solution and partly because the spectra are so complicated. In addition, mono-cationic Pcs and porphyrins have a higher tendency towards aggregation. Thus, it has not been possible to establish trends that relate such variables as temperature,

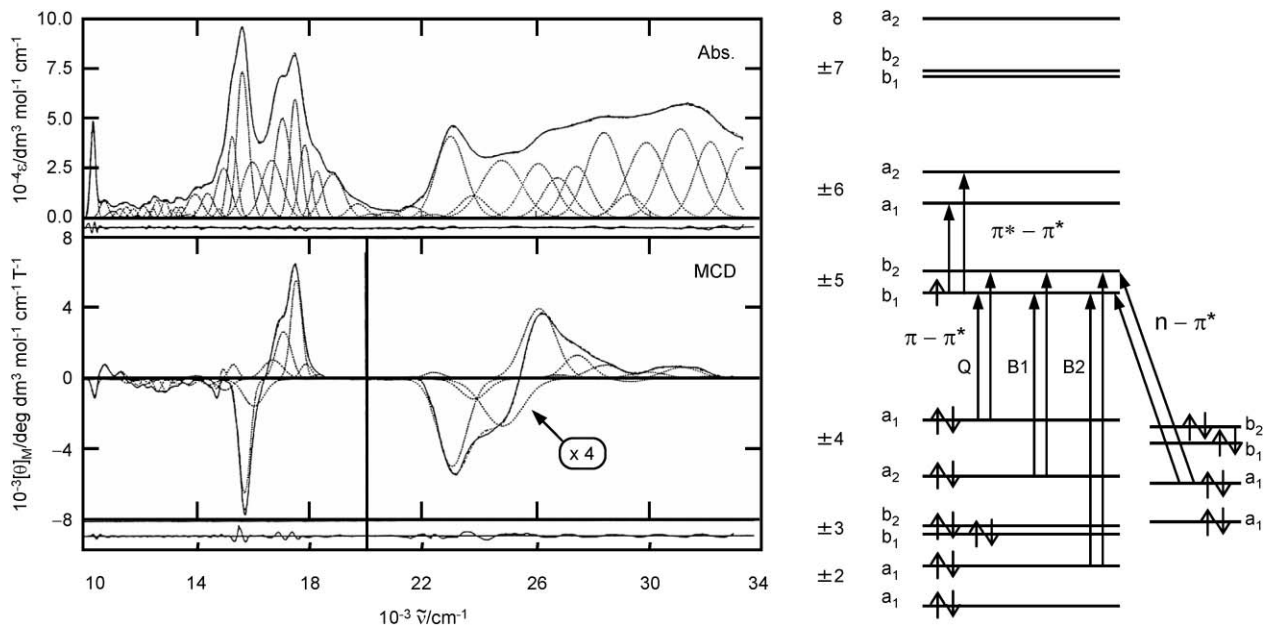

Fig. 11 Absorption and MCD spectra of the ring-reduced anion radical of ZnPc and their band deconvolutions (left), and molecular orbitals involved in the major π–π* and n–π* absorption transitions with energies between 10000 and 35000 cm^{-1} (right) (redrawn from ref. 22). The arrows indicate possible allowed transitions that give rise to bands observed in the 300–900 nm region. The association of orbital angular momentum with pairs of states follows from the assignment of the molecular orbitals of an aromatic ring in terms of orbital angular momentum in the sequence 0, ±1, ±2, *etc*. Note that the Q and B1 bands arise from transitions out of ±4 orbitals into ±5 orbitals and can be associated with an allowed ±1 transition (B1) and a forbidden ±9 transition (Q). New bands are expected for the transition out of the e_g* orbital (in D_{4h} symmetry) that is π*–π* in character. The labels are for the proposed C_{2v} geometry.

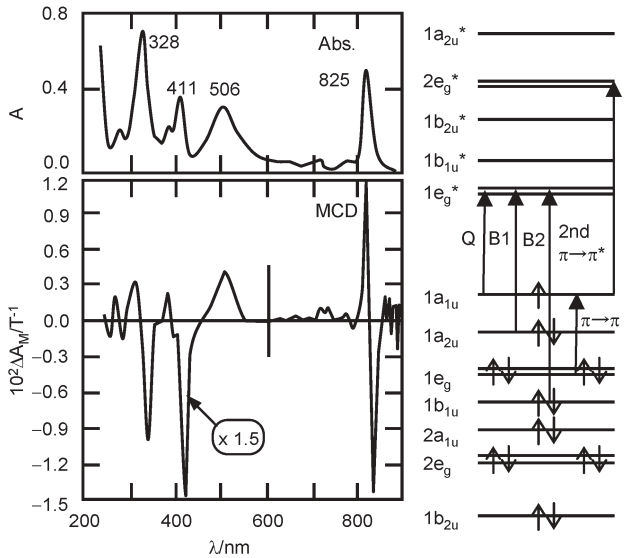

Fig. 12 Absorption and MCD spectra of the ring-oxidized monocation radical of MgPc (left) and molecular orbitals involved in the major π–π* absorption transitions with energies between 10000 and 35000 cm^{-1} (right) (redrawn from ref. 24).

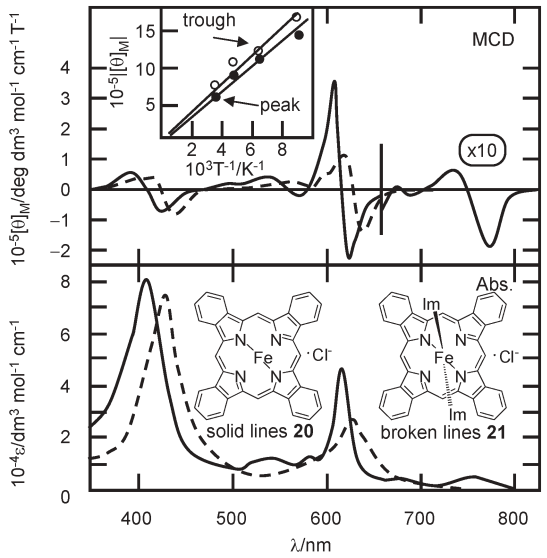

Fig. 13 Absorption and MCD spectra of **20** (solid lines) and **21** (broken lines). The inset shows the temperature dependence of the Q MCD peak and trough of **21** (redrawn from ref. 26*a*).

solvent, axial ligation and central metal to energies and intensities of the individual bands in the spectra. The first reliable absorption and MCD spectra of monomeric monocation-radical species of ZnPc[7] and MgPc[24] were also reported from Stillman's group. An example of a MgPc cation is shown in Fig. 12. As seen clearly, dispersion type *A* terms were recorded corresponding to all transitions except that seen around 500 nm. In total, eight *A* terms were identified between 900 and 250 nm. Thus, with the exception of the 500 nm bands, we can immediately understand that these eight bands correspond to transitions to degenerate excited states. Taking the results of MO calculations into account, the band at 500 nm was assigned to a nondegenerate transition from a low-lying MO into the half-filled a_{1u} (π) MO under D_{4h} symmetry.

(E) Species showing Faraday *C* terms. Normal D_{4h} type metalloporphyrins show Faraday *A* terms in both the Soret and Q band regions, since the ground state is not degenerate while the first excited state is doubly degenerate. However, ferric d^5 low-spin porphyrins show Faraday *C* terms in the Soret, Q and near-IR regions. Here, if we postulate the wavefunctions of these porphyrins as the products of those of the porphyrin π-system and iron, the ground state is doubly degenerate since the fifth d-electron can occupy either degenerate d_{xz} or d_{yz} orbitals. This property was applied to determine the oxidation state of iron in iron tetrabenzoporphyrin (FeTBP). For many years, it was known that the oxidation state of iron in iron porphyrin is +3 under aerobic conditions while that of iron in phthalocyanine is +2. Accordingly, there was an interest in the oxidation state of iron in FeTBP. However, because of the low solubility of this compound, determination by EPR and the Evans method[25] using NMR appeared difficult. In an experiment down to 110 K, FeTBP coordinated by two imidazole groups showed a Q MCD trough and peak whose intensity was proportional to $1/T$ (Fig. 13), confirming that the oxidation state of iron in FeTBP is +3.[26] As shown in the inset of this figure, when extrapolated to infinitely high temperature, the MCD intensity becomes zero, confirming a contribution from only *C* terms. In order for the wavefunctions of ferric low-spin porphyrins to be expressed by the product of those of the porphyrin skeleton and iron, both wavefunctions must mix well, and this in turn needs the iron to lie in the center of the central hole of the porphyrin skeleton. In accordance with this anticipation, in the case of hemoproteins, it is known that iron in the ferric low-spin state lies deep inside the hole, while in the ferric high-spin state, it is positioned above the hole.[27]

The second example of a Faraday *C* term is the near-IR MCD of ferric low-spin cytochrome *c* (Fig. 14).[28] Not only cyctochrome *c*, but also the near-IR bands of ferric hemoproteins have been assigned as charge-transfer transitions from porphyrin a_{1u} and a_{2u} (π) to iron e_g (dπ) orbitals in D_{4h} symmetry. This CT band appears at longer wavelength (*ca.* 1100–2000 nm) than that of ferric high-spin porphyrins (*ca.* 800–1100 nm), since the d_{xz} and d_{yz} levels of low-spin compounds are lower than that of high-spin compounds. The ground state is doubly degenerate if we consider the wavefunction as the product of those of the porphyrin moiety and iron, while the excited state is nondegenerate since both the d_{xz} and d_{yz} orbitals are each occupied by two electrons.[29] Thus, in this case, Gaussian-shaped curves with an intensity proportional to the inverse of the absolute temperature were observed.

In the natural enzymes peroxidase and catalase, there are species named compound I and II intermediates, which are two and one oxidation equivalents above the native ferric (Fe^{III}) heme, respectively. Much of the previous work on these intermediates was undertaken in order to understand the role that these unusual heme electronic structures play in the enzymatic process. In the case of horseradish peroxidase (HRP), spectroscopic studies of compound I indicated that

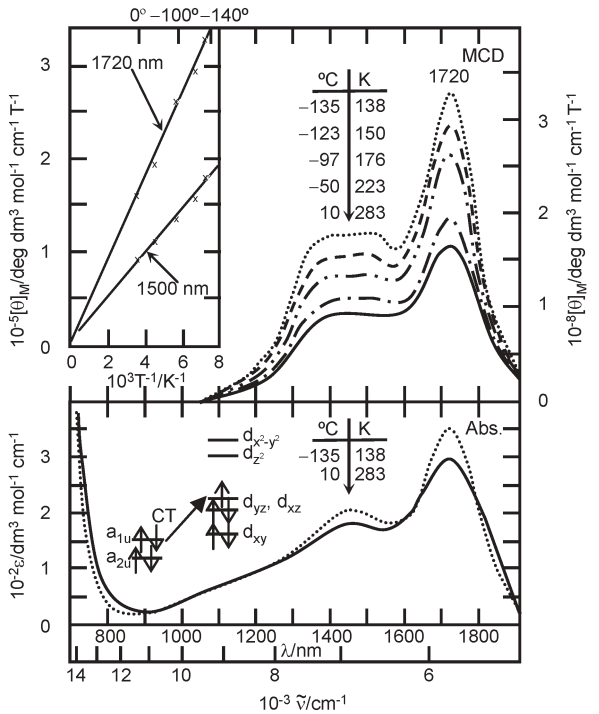

Fig. 14 Absorption and MCD spectra of cytochrome c in the near-IR region (redrawn from ref. 28*a*). The inset shows the temperature dependence of the MCD intensity at two wavelengths. Also, in the figure, note that the energy of a_{1u} and a_{2u} is approximately the same.

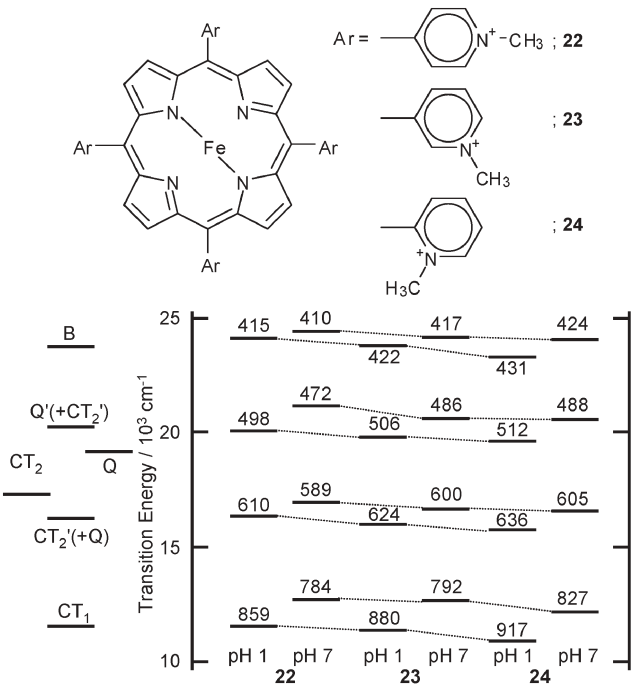

Fig. 15 Band positions of several states of three water-soluble porphyrin isomers **22–24** obtained from electronic absorption and MCD spectra (redrawn from ref. 31*b*). Species at pH 1 and 7 are axially coordinated by one H_2O and OH, respectively. The Q and CT_2 states interact to produce two states CT_2' and Q′, which have more CT_2 and Q character, respectively.

both oxidation equivalents are located on a heme that is in the form of a ferryl (Fe^{IV}) heme π-cation-radical complex. In MCD experiments carried out below 30 K, the temperature-dependent band intensified and finally saturated below 2 K.[30] This temperature-dependence was attributed to the effects of the S = 3/2 Kramer's doublets ground state of the coupled Fe(IV) heme π-cation-radical species. The results of band deconvolution analysis of both MCD and absorption spectra clearly indicated that the ground states in both HRP and catalase compound I species should be considered to be admixtures of the $^2A_{1u}$ and $^2A_{2u}$ configurations, rather than an equilibrium mixture of configurations often used in explanations of the spectroscopic properties of hemoproteins. This kind of explicit interpretation of the electronic states of ferryl hemes had not been possible without use of MCD spectroscopy.

(F) Other examples. The pyridyl nitrogen of *meso*-tetrapyridylporphyrins can be quaternized by methylation, to afford water-soluble porphyrins over the entire pH region. Thus, the iron complexes have been used as model compounds of natural hemes. In addition to π–π* transitions, many CT transitions can be observed in their absorption spectra, similarly to those of natural ferric hemes. However, the energy of these transitions could not necessarily be accurately determined from their absorption spectra due to the often-encountered, integral type broad absorption spectra. By applying MCD spectroscopy, the energies of various transitions of three methylated *meso*-pyridylporphyrin ferric high-spin isomers were determined at neutral and acidic pHs (Fig. 15).[31] Since the CT band in the visible region had been assigned as the transition from b_{2u} (π), a_{2u} (π) to e_g (dπ),[27] this CT state (E_u) could interact with the E_u π–π* excited state. In addition, since the excited state is doubly degenerate, most MCD signals are dispersion-type Faraday *A* terms which afford explicit energies of bands. In Fig. 15, species at neutral pHs are axially coordinated by one OH group and those at pH 1 by one H_2O molecule. Thus, it is evident from this Figure that the position of the pyridyl nitrogen of *meso*-pyridyl groups affects the electronic properties of the porphyrin chromophore, so that the further away the position of the nitrogen, the lower the energy of π–π* and CT states. The position of the pyridyl nitrogen also affects the pH of the transition between the neutral species and the alkaline species coordinated by two OH groups, as well as EPR parameters such as rhombicity.

MCD spectroscopy was also applied as a probe for the distal histidine residue in myoglobin and monomeric hemoglobin. For many years, it has been suggested that the distal histidine has possible roles of acting as a gate or swinging door for ligand entry into the heme pocket and of stabilizing the bound dioxygen by hydrogen-bond formation. Furthermore, to facilitate the effective movement of a catalytic proton from the solvent to coordinated dioxygen *via* the imidazole ring, it participates in a proton-relay mechanism for the autoxidation of oxymyoglobin to its met (Fe^{III}) form. However, it was not easy to determine unequivocally whether or not a myoglobin or a hemoglobin contains the usual histidine residue, even if the amino acid sequence was known. Since the MCD signal in the Soret region had been used as a more direct probe for the

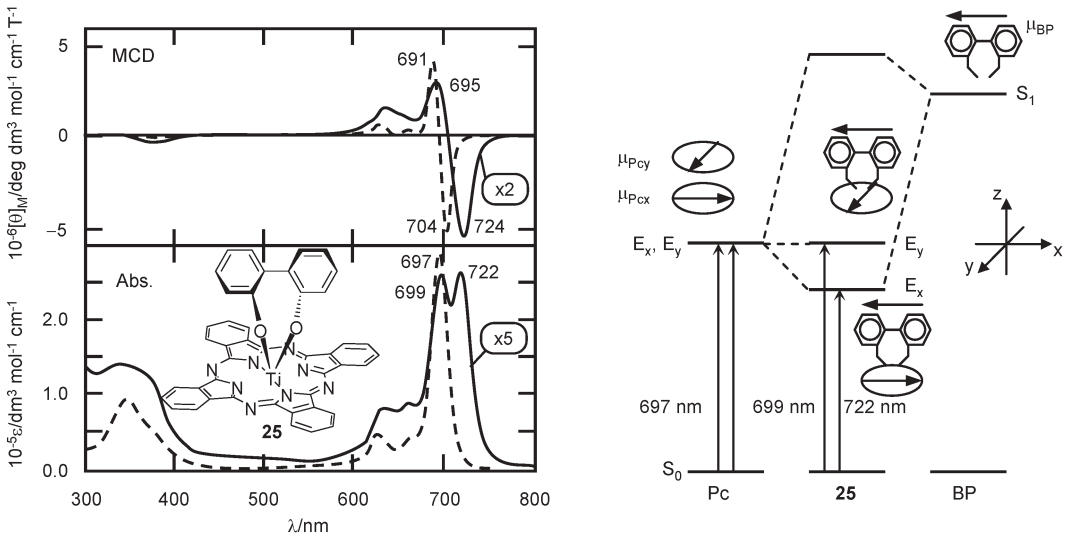

Fig. 16 Absorption and MCD spectra of **25** (left, solid lines) and TiOPc (left, broken lines), and exciton interaction between the Pc and biphenyl (BP) ligands in **25** (right) (redrawn from ref. 35). μ_{Pcx}, μ_{Pcy} and μ_{BP} are the electronic dipole moment of the Q_x transition, of the Q_y transition, and of a transition to S1 of BP, respectively. Only μ_{Pcx} can couple with μ_{BP}, shifting the E_x state to lower energy.

spin states and iron-coordination geometry in a wide variety of hemoproteins,[32] the Soret MCD spectra were compared for ten myoglobins (or monomeric hemoglobins) including the proteins isolated from lower organisms.[33] When Soret absorptivity was mapped against MCD (peak-to-trough) intensity, two islands appeared, of which the one with small absorptivity and MCD intensity was predicted with high accuracy to be a species lacking the distal histidine. In addition to myoglobins from gastropodic sea molluscs, the distal histidine residue was also found to be absent in myoglobins of a shark and a mammalian African elephant (obtained from a dead elephant in a zoo). Since the results were consistent for species lacking the distal histidine from the known amino acid sequence, it was concluded that this method can be applied to species whose amino acid sequence is not known. Similarly, the pH-dependent swing-out of the distal histidine residue in ferric hemoglobin of a midge larva (*Tokunagayusurika Akamushi*) was detected by measuring the Soret MCD intensity associated with pH change.[34]

An interesting case of practical lowering of the chromophore symmetry is seen in the Q band of a biphenyl-linked TiPc (Fig. 16).[35] In this example, the Pc π-system is approximated as D_{4h} symmetry. However, since one of the transition moments in the Q band interacts with the transition moment which is parallel to the Pc plane of biphenyl, the Q band is split by exciton interaction. As a result, the Q band splits to some degree. However, since the amount of splitting is not large, the sum of *B* terms of opposite sign gave a dispersion-type MCD curve called pseudo-Faraday *A* term. Note that the positions of the MCD trough and peak approximately correspond to two absorption peaks in the Q band region (in the case of TiOPc drawn by broken lines, the inflection point of the Q MCD curve corresponds to the absorption maximum).

The last example is an application to triazacorrole (Fig. 17).[36] This compound has C_{2v} symmetry so that all observable signals are Faraday *B* terms which have peaks or troughs associated with absorption peaks. The most important features to note are in the 520–570 nm region. Looking only at the absorption spectra, we cannot assess whether or not this

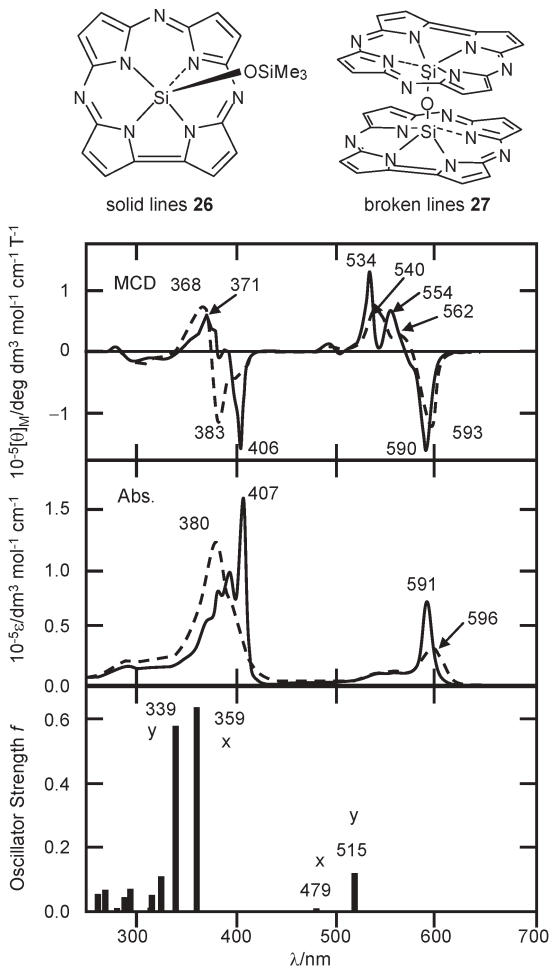

Fig. 17 Absorption and MCD spectra of a triazacorrole **26** and its μ-oxo dimer **27** (redrawn from ref. 36).

region results from vibrational components of the band at 591 nm. However, the MCD spectra of positive sign in the corresponding region clearly indicates that it should be ascribed to another transition, since a negative MCD trough appeared corresponding to the absorption peak at the longest wavelength, which was supported by the MO calculations shown at the bottom of this Figure.

2 Dimers and oligomers

(A) Cofacial dimers. Four-(15-crown-5)-substituted Pcs (CRPc) dimerize when cations such as K^+ or Ca^{2+} are added through a two-step three-stage process to form cofacial eclipsed dimers.[37] Although the X-ray data have not been reported, these are considered to be some of the most perfectly eclipsed dimers (*i.e.* dimers of geometry D_{4h}, Fig. 18, top), of any porphyrins produced to date, while even paracyclophanes have either slipped stack or mutually rotated structures. The spectra of cofacial eclipsed dimers of H_2-, Ni- and ZnCRPc were recorded and analyzed by band deconvolution.[38] All spectra were shifted to shorter wavelengths compared with those of monomers, indicating that they can be explained by an exciton coupling phenomenon. In the case of the NiCRPc dimer, six *A*-terms were confirmed, in contrast to four *A*-terms for the monomer in the 260–700 nm range. Most noteable is the detection of five *A*-terms in the spectra of H_2CRPc (Fig. 18, bottom). Since the constituent H_2CRPc has D_{2h} symmetry, this finding indicates that one of the major effects of cofacial dimerization is to increase the symmetry of the π states, at least to D_{4h}, so that *A*-terms were observed under the main π–π* transitions. This increase in symmetry was further confirmed by using crowned tribenzotetraazaporphyrin with C_{2v} symmetry.[39] When cofacial dimers of geometry C_{2v} were formed by the addition of cations, these still showed Faraday *A* terms corresponding to the Q absorption peaks, so that it was concluded that *the spectra of cofacial eclipsed dimers do not reflect the molecular symmetry of the constituent monomers* (or chromophores).

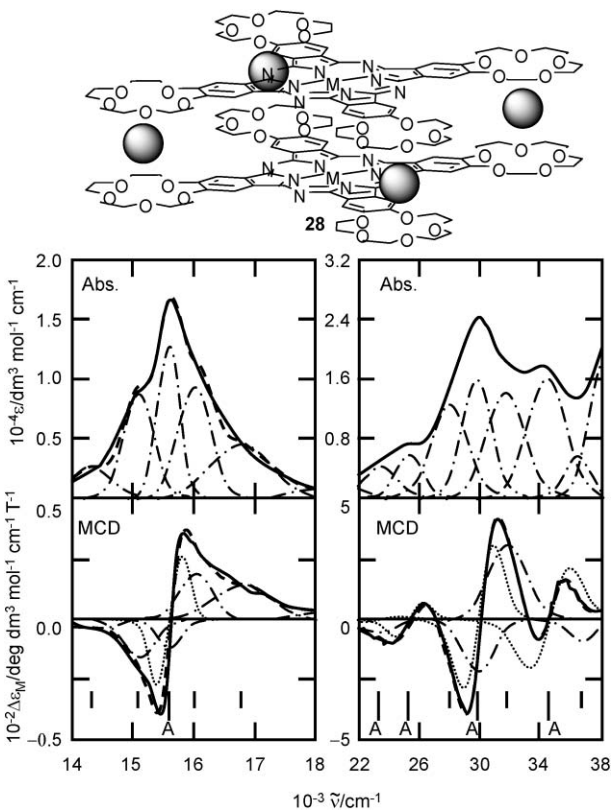

Fig. 18 Band deconvolution analysis of the absorption and MCD spectra of a metal-free (M = H_2) 15-crown-5 Pc cofacial eclipsed dimer **28** obtained by addition of K^+ (redrawn from ref. 38). The shaded circle represents the K^+ ion. The positions of *A* terms are indicated.

Ishikawa and co-workers analyzed the electronic and MCD spectra of several sandwich type Pc complexes.[40] In the homoleptic complexes with closed-shell systems, the 1st and 2nd excited states are doubly degenerate, so that transitions to these states which appear in the Q band region should produce Faraday *A* MCD terms. In the case of the lanthanide sandwich complexes, the band to the longest wavelength has a weaker intensity than the second band. These two bands lie at longer and shorter wavelength, respectively, of the Q_{00} band of the constituent monomer. The splitting energy of these two bands depends sensitively on the ionic size, decreasing markedly with increasing ionic radius.[41] These observations, two Faraday *A* MCD terms corresponding to these two absorption peaks, together with theoretical calculations allowed the author to conclude that the transitions to the lowest excited state contain a charge resonance configuration as a main component, while the transitions producing the second band from lower energy have exciton terms as the dominant component.[40c] Charge resonance in such systems refers to, with a localized orbital basis (valence bond method), the HOMO to LUMO transitions between different chromophore units, while exciton terms are those in the same chromophore units. These spectral features were also observed for SnPc sandwich[40a] and Lu pyrazinoporphyrazine double decker complexes (Fig. 19).[42]

The lanthanide Pc double decker complex has, in the neutral oxidation state ($[Ln^{III}(Pc)_2]^0$), a hole in the π-system of the Pc ring(s). Absorption spectra of the complexes resemble a

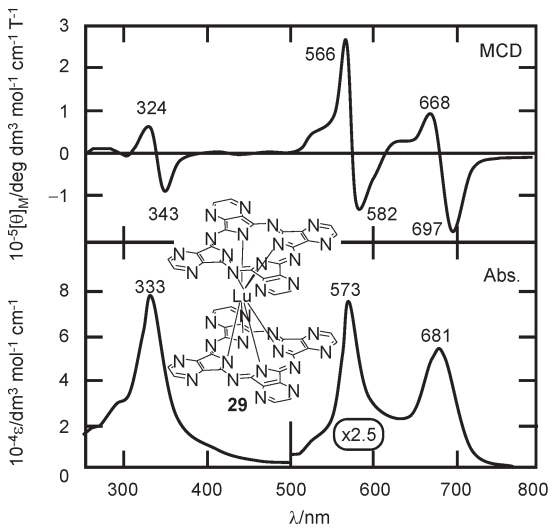

Fig. 19 Absorption and MCD spectra of the pyrazinoporphyrazine–lutetium sandwich dimer (redrawn from ref. 42).

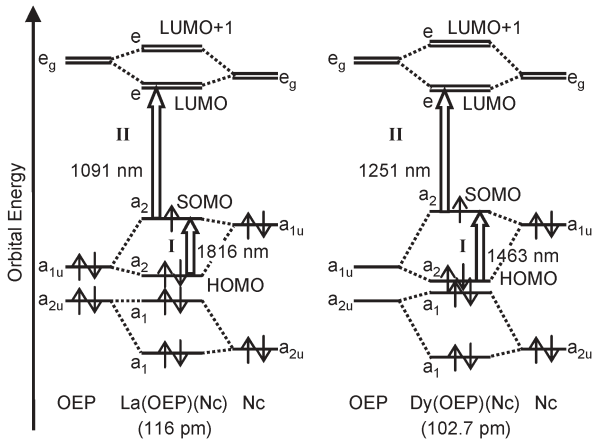

Fig. 20 Schematic representation of the frontier MO energies for the C_{4v} sandwich dimers La(OEP)(Nc) **30** (left) and Dy(OEP)(Nc) **31** (right) (redrawn from ref. 43). The value in parentheses indicates the size of the central metal.

superimposition of those of neutral and cation radical monomers. For example, $Lu(Pc)_2$ shows absorption bands at 15200 (*ca.* 660 nm) and about 30000 cm^{-1} (*ca.* 330 nm) which can be regarded as those of a neutral monomer ($M^{II}(Pc)$ or Pc^{2-}), and at 11000 (*ca.* 910 nm) and 22000 cm^{-1} (*ca.* 450 nm) which can be attributed to a cation radical ($M^{II}(Pc)^{+}$ or Pc^{-}). In addition, a new band appears at 7000 cm^{-1} (*ca.* 1430 nm) which does not belong to either Pc^{2-} or Pc^{-}.[40b] Although these bands could be assigned by taking the MCD and MO calculation results into account,[40e] the correctness of the assignments were confirmed through experimental MCD data of heteroleptic sandwiches described subsequently.

The assignment of absorption bands of heteroleptic double decker complexes appeared further difficult, since each band consists of non-equal contributions from each of the two chromophore units. Jiang and co-workers prepared a series of OEP-Nc rare-earth sandwich complexes. Luckily, even the ionic size was different, all compounds had staggered conformations (confirmed by X-ray crystallography) so that the spectral difference could be analyzed only by considering the interplanar distance of two chromophores as a parameter.[43] Fig. 20 shows a schematic representation of the frontier MO energies for the D_{4d} sandwich dimer (Mt(OEP)(Nc)) with larger (Mt = La) and smaller (Mt = Dy) central metals, together with observed wavelengths of the two absorption bands to the lowest energy. Band I lying at the longest wavelength (*ca.* 1340–1820 nm) was assigned as a transition from the HOMO to a singly occupied MO (SOMO). This band shifts to shorter wavelength with decreasing ionic radius of the metal, since the splitting of the HOMO and SOMO increases. Band II (1090–1340 nm), which was assigned to a transition from the SOMO to doubly degenerate LUMO, shifts to longer wavelength with decreasing size of the central metal, since the energy difference between the HOMO and SOMO and that between the LUMO and LUMO+1 becomes larger, giving rise to a smaller SOMO–LUMO gap. Although the above assignments are mainly based on the shift of the bands due to ionic size, if they are correct, MCD should give a *B* and *A* term, respectively, corresponding to bands I and II. As shown in Fig. 21, Faraday *B* and *A* terms were indeed observed associated with bands at the longest and second longest wavelength, although the *B* term is very weak in this scale. The correctness of the band assignments was also confirmed by measuring the spectra of both the reduced and oxidized species. When an electron is added to the SOMO, band I disappears since the SOMO is occupied by two electrons to become the HOMO, and Faraday *A* MCD terms are observed corresponding to almost all absorption peaks, since the excited states are often doubly degenerate. In contrast, when an electron is removed from the SOMO by oxidation, band II disappears, as can be easily concluded from Fig. 20.

(B) Cofacial trimers. Theoretical consideration of the electronic states of trimers has been also carried out by Ishikawa.[40g,h,k] However, MCD spectra of all regions were not reported due to instrumental limitation, since some bands appeared in the near-IR region. We have succeeded in

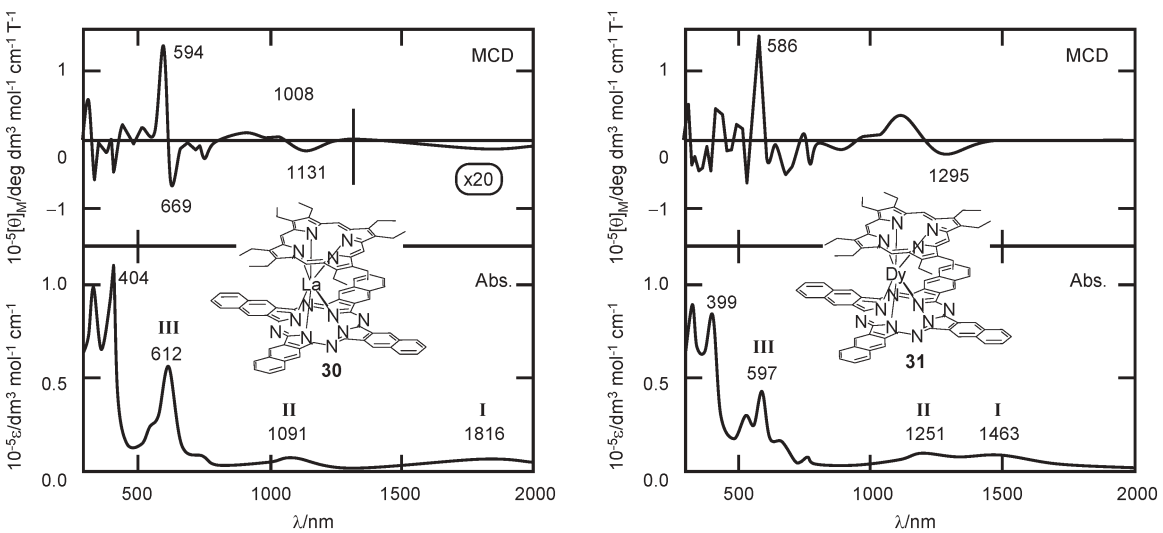

Fig. 21 Absorption and MCD spectra of La(OEP)(Nc) **30** and Dy(OEP)(Nc) **31** heteroleptic sandwiches (redrawn from ref. 43).

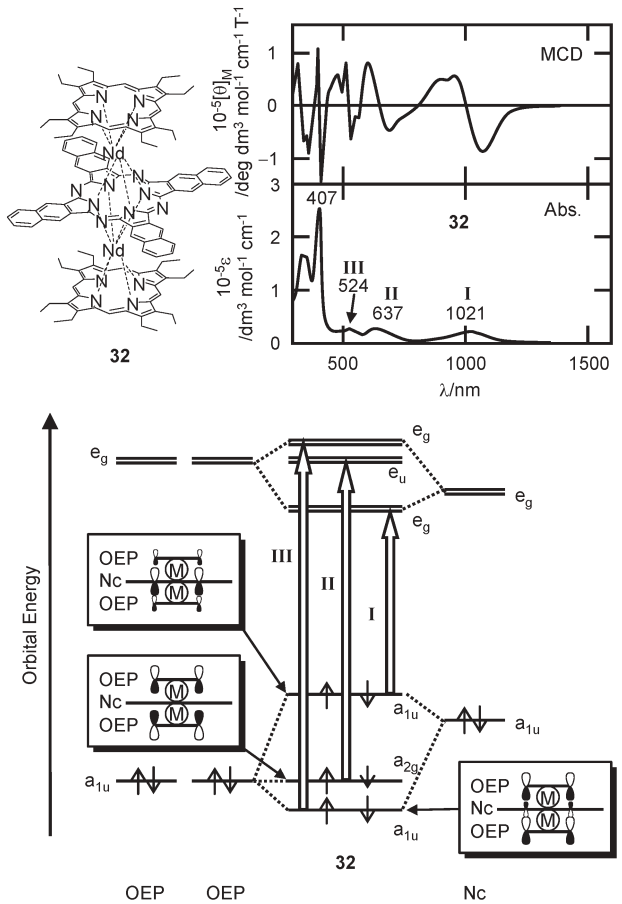

Fig. 22 Absorption and MCD spectra (top) of an (OEP)(Nc)(OEP) sandwich trimer of neodymium **32** with D_{4h} symmetry, and a schematic representation of its frontier MO energy levels (bottom) (redrawn from ref. 43).

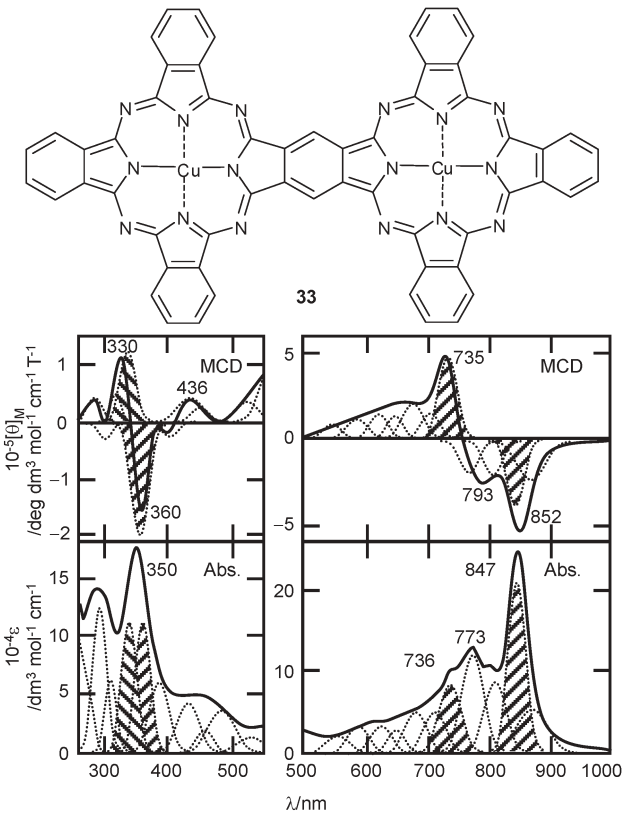

Fig. 23 Absorption and MCD spectra of a planar Pc dimer **33** and band deconvolution analysis of these (redrawn from ref. 45). The shaded components are the split components in the Q and Soret band regions.

definitively assigning some absorption bands of triple deckers consisting of two trivalent lanthanide ions, two OEP rings and an Nc ring (Fig. 22). In this species, no radical is included, and all the MCD signals corresponding to absorption peaks can be clearly attributed to *A* terms because of the first derivative type shapes. Fig. 22 (bottom) indicates a schematic MO energy diagram for the triple-decker system. As with the experimental observations, with decreasing metal size, the absorption peak of Band I shifts considerably to longer wavelength, while that of Bands II and III show little or no variation. This feature is consistent with the diagram. The HOMO of the trimer arises from the antibonding interaction of the a_{1u} orbitals of the three π orbitals, and the Nc ring has the largest MO coefficients. In contrast to the HOMO, the Nc plane becomes a node in the case of HOMO−1, so that the interaction energy is considered to be small. The HOMO−2 should be composed primarily of OEP orbitals, and thus is stabilized because of the bonding interaction of the three chromophores.

(C) Planar dimers of azaporphyrins. Planar Pc homodimers sharing a common benzene ring were first prepared by Leznoff *et al.*,[44] and a dicopper complex analyzed by electronic absorption and MCD using the band deconvolution technique (Fig. 23).[45] Since the molecular symmetry was D_{2h}, the splitting of the Q band was anticipated. However, as this figure shows, a notable finding was that the second intense band in the Q band region at 773 nm does not correspond to one of the split components. If we utilize the MCD property that interacting transitions give *B* terms of opposite sign, it is easily understandable that a shoulder at 736 nm corresponds to this split component. By band deconvolution analysis, the intensity ratio of the Q_x : Q_y and $(Soret)_x$: $(Soret)_y$ bands were experimentally found to be *ca.* 2 : 1 and 4 : 5, respectively, and surprisingly, these ratios were almost perfectly reproduced later by independent PPP MO calculations.

Spectral and electrochemical properties of heteroleptic planar Pc–pyrazinoporphyrazine and Pc–Nc dimers have also been examined.[46] Although their molecular structure is similar to that of the homodimers, their Q bands were different in shape, being commonly composed of two peaks at around 800–900 and 650–750 nm. The former is sharp while the latter is round and broad, suggesting that the latter peak contains a plurality of transitions. Corresponding to these bands, a negative MCD trough (*B* term) and a dispersion type pseudo *A* term were recorded, respectively (Fig. 24). Accordingly, MO calculations were performed in order to gain insight into the difference. As a result, it was found that two energetically close transitions were included in the broad absorption peak of heteroleptic dimers, in good contrast to the single transition of homoleptic dimers. Thus, this type of difference in spectral origin was experimentally easily detectable only by MCD.

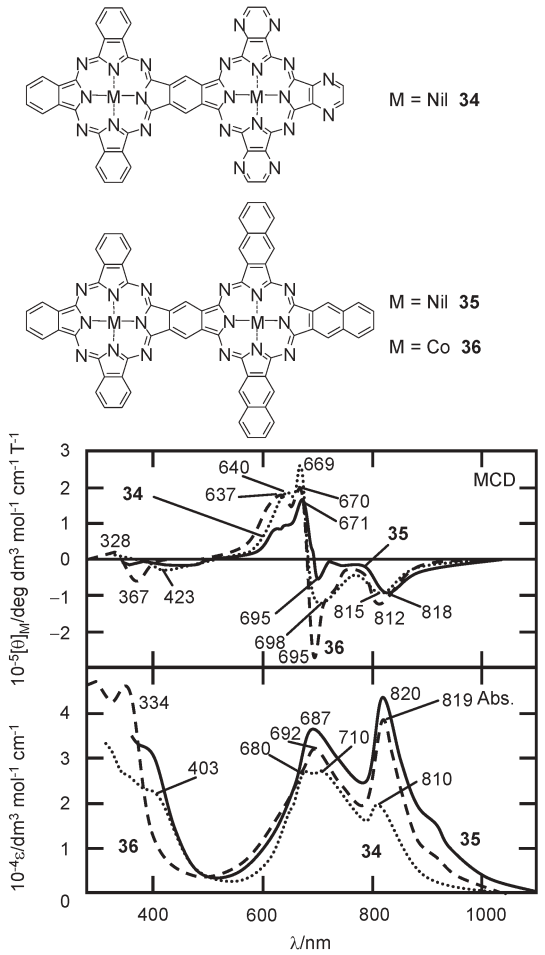

Fig. 24 Absorption and MCD spectra of deprotonated planar PcPyz **34** (dotted lines) and PcNc **35** (solid lines), and the dicobalt derivative **36** of PcNc (redrawn from ref. 46). Note that pseudo Faraday *A* MCD terms are observed in the *ca.* 650–750 nm region.

(D) Planar oligomers of porphyrins. We introduce here two examples. Absorption and MCD spectra of a series of rectangular planar porphyrin oligomers fused by two or three covalent bonds were analyzed.[47] Fig. 25 shows the spectra of oligomers connected by three bonds, together with those of a reference monomer. In the oligomers, the Soret and Q bands split, and the latter band intensifies and spreads into the near-IR region. Since these compounds are approximated by D_{2h} symmetry, both the Soret and Q bands split into at least two peaks (the Soret band region is complex, since several transitions are included). The relative intensity of the Q band to the Soret band increases with increasing number of constituting porphyrin units. All oligomers showed positive MCD envelopes of *B* terms corresponding to the absorption peaks at the longest wavelength (QI in the Figure). According to MCD theory, a negative MCD *B* term envelope should appear corresponding to the split Q absorption peak, which is not clear in the present system. We found this peak as a tiny shoulder or peak on the lower energy side of the split Soret peak (QII in the Figure) by inspection of the absorption spectra. In the Soret band region, a negative and a positive MCD *B* term appeared, corresponding to the two intense split absorption peaks. Since the MCD sign changes plus-to-minus in ascending energy in the Q band region, it was predicted from MCD theory that the energy difference between the HOMO and HOMO−1 (ΔHOMO) is smaller than that between the LUMO and LUMO+1 (ΔLUMO). This was reproduced for all the oligomers by MO calculations using the TDDFT method. In addition, the calculated intensity of the QII band was about 1/15 of that of QI, in agreement with the very weak QII band intensity in this Figure.

The 2nd case in this category is a square planar porphyrin tetramer in which the rings are connected to each other by three covalent bonds (Fig. 26).[48] When this compound was synthesized, the ring current effect normally seen for aromatic

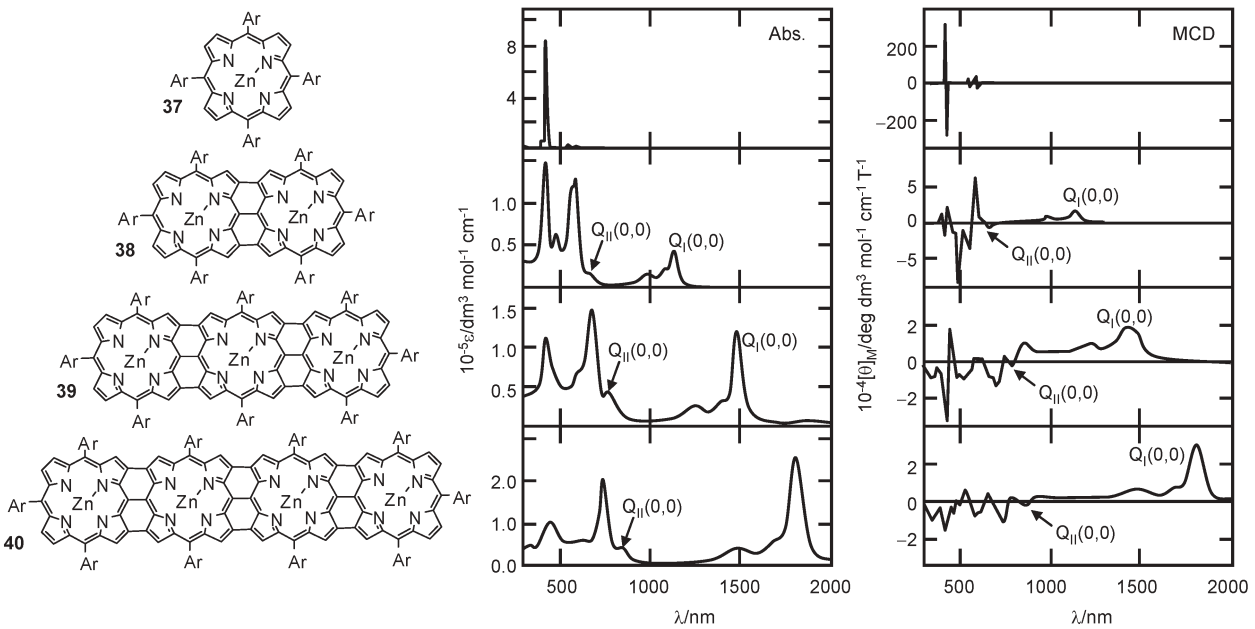

Fig. 25 Absorption and MCD spectra of porphyrins **37–40** (redrawn from ref. 47). Q_I and Q_{II} indicate long-axis and short-axis polarized transitions, respectively.

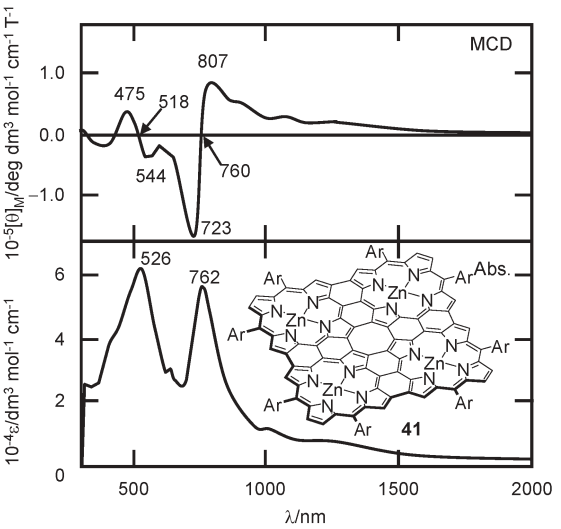

Fig. 26 Absorption and MCD spectra of the square porphyrin tetramer **41** (redrawn from ref. 48).

compounds was not detected in its ^{1}H NMR spectrum. The electronic absorption spectrum of this species was also strange (Fig. 26), consisting of strong peaks at 526 and 762 nm accompanied by weak, broad absorptions extending into the near-IR region. This absorption spectrum has been simulated using time-dependent Hartree–Fock theory based on the ZINDO/S Hamiltonian. Two intense bands were predicted for the experimental 525 and 762 nm bands, and the predicted excited states were doubly degenerate E_u, leading to a prediction of Faraday *A* MCD terms. The observed *A* term was negative for the absorption band at 762 nm, indicating that the ΔLUMO is larger than ΔHOMO. The MO calculations revealed that the 762 nm band arises from a transition linking a degenerate orbital with a nondegenerate one, whereas the 526 nm band arises primarily from a transition linking a nondegenerate orbital and a degenerate one. Negative Faraday *A* terms tend to arise from transitions in which orbital angular momentum (OAM) is greater in the ground state than in the excited state, while positive Faraday *A* terms are associated with transitions where OAM is greater in the excited state. Because the OAM associated with electron circulation would normally be anticipated to be greater within a degenerate orbital, the results obtained from the calculations were considered to be consistent with the positive and negative Faraday *A* terms observed for the 526 and 762 nm bands, respectively.

Concluding remarks

In this mini-review, we have introduced some representative papers on the MCD spectroscopy of porphyrinoids. The technique is sensitive to the spin and oxidation states of the central metal and the symmetry of the ligand. Although MCD spectroscopy is often overlooked, in many instances it has provided key information required to successfully assign the absorption bands of chromophores, which cannot be derived from a consideration of only the electronic absorption spectrum and the results of MO calculations. For example in the case of the research of Osuka and co-workers on zinc porphyrin dimers,[49] analysis of MCD spectral data was required to definitively assign the absorption bands in the near-IR region.[47] In future it would be desirable if researchers within the field could calculate MCD spectra based on TD-DFT using commercially available software packages in the same manner that they currently calculate electronic absorption spectra. Seth *et al.*[50] have reported the first examples of calculations of the Faraday terms in this regard. Even in the absence of modern DFT based calculations, however, we firmly believe that an MCD analysis based on semi-empirical approaches such as Gouterman's 4-orbital model[51] and Michl's perimeter model[3b] should still be regarded as an essential component of any assignment of the optical spectra of the porphyrinoids.

References

1 (*a*) B. Holmquist, in *The Porphyrins*, ed. D. Dolphin, Academic Press, New York, 1978, vol. 3, pp. 249–270; (*b*) M. J. Stillman and T. Nyokong, in *Phthalocyanines—Properties and Applications*, ed. C. C. Leznoff and A. B. P. Lever, VCH, Weinheim, New York, 1989, vol. 1, ch. 3; (*c*) J. H. Dawson and D. M. Dooley, in *Iron Porphyrins*, ed. A. B. P. Lever and H. B. Gray, VCH, Weinheim, New York, 1989, Part III, pp. 1–135; (*d*) M. J. Stillman, in *Phthalocyanines—Properties and Applications*, ed. C. C. Leznoff and A. B. P. Lever, VCH, Weinheim, New York, 1993, vol. 3, ch. 5; (*e*) J. Cheek and J. H. Dawson, in *The Porphyrin Handbook*, ed. K. M. Kadish, R. Guilard and K. M. Smith, Academic Press, New York, 2000, vol. 7, ch. 53; (*f*) J. Mack and M. J. Stillman, in *The Porphyrin Handbook*, ed. K. M. Kadish, R. Guilard and K. M. Smith, Academic Press, New York, 2003, vol. 16, ch. 103.

2 (*a*) P. N. Schatz, A. J. McCaffery, W. Suetaka, G. N. Henning, A. B. Ritchie and P. J. Stephens, *J. Chem. Phys.*, 1966, **45**, 722; (*b*) G. N. Henning, A. J. McCaffery, P. N. Schatz and P. J. Stephens, *J. Chem. Phys.*, 1968, **48**, 5656.

3 (*a*) A. Kaito, A. Tajiri and M. Hatano, *J. Am. Chem. Soc.*, 1975, **97**, 5069; (*b*) A. Castellan and J. Michl, *J. Am. Chem. Soc.*, 1978, **100**, 6824, and 14 companion papers in the same issue.

4 (*a*) *The Porphyrin Handbook*, ed. K. M. Kadish, R. Guilard and K. M. Smith, Academic Press, New York, 2000, vol. 1 and 2; (*b*) N. Kobayashi, in *Phthalocyanines—Properties and Applications*, ed. C. C. Leznoff and A. B. P. Lever, VCH, Weinheim, New York, 1993, vol. 2, ch. 3; (*c*) N. Kobayashi, *The Porphyrin Handbook*, ed. K. M. Kadish, R. Guilard and K. M. Smith, Academic Press, New York, 2003, vol. 15, ch. 100.

5 (*a*) J. Michl, *Pure Appl. Chem.*, 1980, **52**, 1549; (*b*) J. Mack, M. J. Stillman and N. Kobayashi, *Coord. Chem. Rev.*, 2007, **251**, 429.

6 N. Kobayashi, S. Nakajima and T. Osa, *Chem. Lett.*, 1992, 2415.

7 T. Nyokong, Z. Gasyna and M. J. Stillman, *Inorg. Chem.*, 1987, **26**, 1087.

8 (*a*) N. Kobayashi, T. Ashida, T. Osa and H. Konami, *Inorg. Chem.*, 1994, **33**, 1735; (*b*) N. Kobayashi, H. Miwa, H. Isago and T. Tomura, *Inorg. Chem.*, 1999, **38**, 479; (*c*) H. Miwa and N. Kobayashi, *Chem. Lett.*, 1999, 1303; (*d*) N. Kobayashi, H. Miwa and V. N. Nemykin, *J. Am. Chem. Soc.*, 2002, **124**, 8007; (*e*) N. Kobayashi and T. Fukuda, *J. Am. Chem. Soc.*, 2002, **124**, 8021; (*f*) N. Kobayashi, J. Mack, K. Ishii and M. J. Stillman, *Inorg. Chem.*, 2002, **41**, 5350; (*g*) H. Miwa, K. Ishii and N. Kobayashi, *Chem. Eur. J.*, 2004, **10**, 4422; (*h*) K. Ishii, H. Itoya, H. Miwa, M. Fujitsuka, O. Ito and N. Kobayashi, *J. Phys. Chem.*, 2005, **109**, 5781.

9 N. Kobayashi and H. Konami, in *Phthalocyanines—Properties and Applications*, ed. C. C. Leznoff and A. B. P. Lever, VCH, Weinheim, New York, 1996, vol. 4, ch. 9. The premise that flat square planar C_{2v} type compounds do not show split absorption band was predicted independently more than 40 years ago by Ballhausen[10a] and Gouterman[10b].

10 (*a*) J. J. Ballhausen, *Introduction to Ligand Field Theory*, McGraw-Hill, New York, 1962; (*b*) M. Gouterman, *J. Mol. Spectrosc.*, 1961, **6**, 138.

11 Abbreviations in this study. HOMO, highest occupied molecular orbital; HRP, horseradish peroxidase; LUMO, lowest unoccupied molecular orbital; MLCT, metal to ligand charge-transfer; Nc, naphthalocyanine; OAM, orbital angular momentum; OEP, octaethylporphyrin; Pc, phthalocyanine; PPP, Parsier–Parr–Pople; Pyz, pyradinoporphyrazine; SOMO, singly occupied molecular orbital; subAP, subazaporphyrin; subNc, subnaphthalocyanine; SubP, subporphyrin; SubPc, subphthalocyanine; TAP, tetraazaporphyrin; TBP, tetrabenzoporphyrin; TDDFT, time-dependent density functional theory; TPP, *meso*-tetraphenylporphyrin; ZINDO, Zerner's intermediate neglect of differential overlap.

12 (*a*) H. Miwa, E. A. Makarova, K. Ishii, E. A. Luk'yanets and N. Kobayashi, *Chem. Eur. J.*, 2002, **8**, 1082; (*b*) T. Fukuda, E. A. Makarova, E. A. Luk'yanets and N. Kobayashi, *Chem. Eur. J.*, 2004, **10**, 117; (*c*) E. A. Makarova, T. Fukuda, E. A. Luk'yanets and N. Kobayashi, *Chem. Eur. J.*, 2005, **11**, 1235.

13 (*a*) E. A. Ough and M. J. Stillman, *Inorg. Chem.*, 1994, **33**, 573; (*b*) E. A. Ough and M. J. Stillman, *Inorg. Chem.*, 1995, **34**, 4317.

14 T. Fukuda, S. Homma and N. Kobayashi, *Chem. Commun.*, 2003, 1574.

15 J. Mack, Y. Asano, N. Kobayashi and M. J. Stillman, *J. Am. Chem. Soc.*, 2005, **127**, 17697.

16 (*a*) N. Kobayashi, *J. Chem. Soc., Chem. Commun.*, 1991, 1203; (*b*) N. Kobayashi, T. Ishizaki, K. Ishii and H. Konami, *J. Am. Chem. Soc.*, 1999, **121**, 9096; (*c*) J. R. Stork, J. J. Brewer, T. Fukuda, J. P. Fitzgerald, G. T. Yee, A. Y. Nazalenko, N. Kobayashi and W. S. Durfee, *Inorg. Chem.*, 2006, **45**, 6148.

17 K. Nakai, K. Kurotobi, A. Osuka, M. Uchiyama and N. Kobayashi, *J. Inorg. Biochem.*, submitted.

18 N. Kobayashi, Y. Takeuchi and A. Matsuda, *Angew. Chem., Int. Ed.*, 2007, **46**, 758.

19 G. Closs and L. Closs, *J. Am. Chem. Soc.*, 1963, **85**, 818.

20 A. P. Boborovskii and V. E. Kholmogorov, *Russ. J. Phys. Chem.*, 1973, **47**, 983.

21 J. G. Lanese and G. S. Wilson, *J. Electrochem. Soc.*, 1972, **119**, 1038.

22 J. Mack and M. J. Stillman, *J. Am. Chem. Soc.*, 1994, **116**, 1292.

23 J. Mack, N. Kobayashi and M. J. Stillman, *J. Porphyrins Phthalocyanines*, 2006, **10**, 1219.

24 E. Ough, Z. Gasyna and M. J. Stillman, *Inorg. Chem.*, 1991, **30**, 2301.

25 D. S. Evans, *J. Chem. Soc.*, 1959, 2003.

26 (*a*) N. Kobayashi, M. Koshiyama and T. Osa, *Chem. Lett.*, 1983, 163; (*b*) N. Kobayashi, M. Koshiyama and T. Osa, *Inorg. Chem.*, 1983, **24**, 2502.

27 D. W. Smith and R. J. P. Williams, *Struct. Bonding (Berlin)*, 1970, **7**, 1.

28 (*a*) N. Kobayashi, T. Nozawa and M. Hatano, *Bull. Chem. Soc. Jpn.*, 1981, **54**, 919; (*b*) T. Yamamoto, T. Nozawa, N. Kobayashi and M. Hatano, *Bull. Chem. Soc. Jpn.*, 1982, **55**, 3059.

29 In contrast, ferric high-spin species show Faraday *A* term corresponding to this CT band, since the excited state is doubly degenerate, *i.e.* in the excited state, one of the d_{xz} and d_{yz} orbitals is singly occupied by an electron. An example of this *A* term is illustrated by FeTBP coordinated with a Cl^- ion in Fig. 13 at around 760 nm.

30 W. P. Browett, Z. Gasyna and M. J. Stillman, *J. Am. Chem. Soc.*, 1988, **110**, 3633.

31 (*a*) N. Kobayashi, M. Koshiyama, T. Osa and T. Kuwana, *Inorg. Chem.*, 1983, **22**, 3608; (*b*) N. Kobayashi, *Inorg. Chem.*, 1985, **24**, 3324.

32 (*a*) L. Vickery, T. Nozawa and K. Sauer, *J. Am. Chem. Soc.*, 1976, **98**, 343; (*b*) A. M. Bracete, M. Sono and J. H. Dawson, *Biochim. Biophys. Acta*, 1991, **1080**, 264.

33 A. Matsuoka, N. Kobayashi and K. Shikama, *Eur. J. Biochem.*, 1992, **210**, 337.

34 K. Akiyama, M. Fukuda, N. Kobayashi, A. Matsuoka and K. Shikama, *Biochim. Biophys. Acta*, 1994, **1208**, 306.

35 N. Kobayashi, A. Muranaka and K. Ishii, *Inorg. Chem.*, 2000, **39**, 2256.

36 N. Kobayashi, M. Yokoyama, A. Muranaka and A. Ceulemans, *Tetrahedron Lett.*, 2004, **45**, 1755.

37 N. Kobayashi and A. B. P. Lever, *J. Am. Chem. Soc.*, 1987, **109**, 7433.

38 Z. Gasyna, N. Kobayashi and M. J. Stillman, *J. Chem. Soc., Dalton Trans.*, 1989, 2397.

39 N. Kobayashi, M. Togashi, T. Osa, K. Ishii, S. Yamauchi and H. Hino, *J. Am. Chem. Soc.*, 1996, **118**, 1073.

40 (*a*) O. Ohno, N. Ishikawa, H. Matsuzawa, Y. Kaizu and H. Kobayashi, *J. Phys. Chem.*, 1989, **93**, 1713; (*b*) N. Ishikawa, O. Ohno and Y. Kaizu, *Chem. Phys. Lett.*, 1991, **180**, 51; (*c*) N. Ishikawa, O. Ohno, Y. Kaizu and H. Kobayashi, *J. Phys. Chem.*, 1992, **96**, 8832; (*d*) N. Ishikawa and Y. Kaizu, *Chem. Phys. Lett.*, 1993, **203**, 472; (*e*) N. Ishikawa, O. Ohno and Y. Kaizu, *J. Phys. Chem.*, 1993, **97**, 1004; (*f*) N. Ishikawa and Y. Kaizu, *Chem. Phys. Lett.*, 1994, **228**, 625; (*g*) N. Ishikawa and Y. Kaizu, *Chem. Phys. Lett.*, 1995, **236**, 50; (*h*) N. Ishikawa and Y. Kaizu, *J. Phys. Chem.*, 1996, **100**, 8722; (*i*) N. Ishikawa and Y. Kaizu, *Chem. Lett.*, 1998, 183; (*j*) N. Ishikawa and Y. Kaizu, *Inorg. Chem.*, 1999, **38**, 3173; (*k*) N. Ishikawa and Y. Kaizu, *J. Porphyrins Phthalocyanines*, 1999, **3**, 514; (*l*) N. Ishikawa, *J. Porphyrins Phthalocyanines*, 2001, **5**, 87.

41 See Fig. 2 in: N. Kobayashi, *Coord. Chem. Rev.*, 2002, **227**, 129.

42 N. Kobayashi, J. Rizhen, S. Nakajima, T. Osa and H. Hino, *Chem. Lett.*, 1993, 185.

43 A. Muranaka, Y. Matsumoto, M. Uchiyama, J. Jiang, Y. Bian, A. Ceulemans and N. Kobayashi, *Inorg. Chem.*, 2005, **44**, 3818.

44 (*a*) C. C. Leznoff, H. Lam, S. M. Marcuccio, W. A. Nevin, P. Janda, N. Kobayashi and A. B. P. Lever, *J. Chem. Soc., Chem. Commun.*, 1987, 699; (*b*) N. Kobayashi, H. Lam, W. A. Nevin, P. Janda, C. C. Leznoff, T. Koyama, A. Monden and H. Shirai, *J. Am. Chem. Soc.*, 1994, **116**, 879.

45 N. Kobayashi, T. Fukuda and N. Kobayashi, *Inorg. Chem.*, 2000, **39**, 3623.

46 N. Kobayashi and H. Ogata, *Eur. J. Inorg. Chem.*, 2004, 906.

47 A. Muranaka, M. Yokoyama, Y. Matsumoto, M. Uchiyama, A. Tsuda, A. Osuka and N. Kobayashi, *ChemPhysChem*, 2005, **6**, 171.

48 Y. Nakamura, N. Aratani, H. Shinikubo, A. Takagi, T. Kawai, T. Matsumoto, Z. S. Yoon, D. Y. Kim, T. K. Ahn, D. Kim, A. Muranaka, N. Kobayashi and A. Osuka, *J. Am. Chem. Soc.*, 2006, **128**, 4119.

49 T. Miyahara, H. Nakatsuji, J. Hasegawa, A. Osuka, N. Aratani and A. Tsuda, *J. Chem. Phys.*, 2002, **117**, 11196.

50 M. Seth, T. Ziegler, A. Banerjee, J. Autschbach, S. J. A. van Gisbergen and E. J. Baerends, *J. Chem. Phys.*, 2004, **120**, 10942.

51 (*a*) M. Gouterman, G. H. Wagniere and L. C. Synder, *J. Mol. Spectrosc.*, 1963, **11**, 108; (*b*) C. Weiss, Jr., H. Kobayashi and M. Gouterman, *J. Mol. Spectrosc.*, 1965, **16**, 415; (*c*) A. J. McHugh, M. Gouterman and C. Weiss, Jr., *Theor. Chim. Acta*, 1972, **24**, 346; (*d*) A. M. Schaffer, M. Gouterman and E. R. Davidson, *Theor. Chim. Acta*, 1973, **30**, 9.

